On improving physical selectivity in the treatment of cancer: A systems modelling and optimisation approach

Haas, O.C.L; Burnham, K.J. and Mills, J.A.

Original citation:
Haas, O.C.L; Burnham, K.J. and Mills, J.A. (1997) On improving physical selectivity in the treatment of cancer: A systems modelling and optimisation approach *Control Engineering Practice* 5 (12), 1739–1745. DOI: 10.1016/S0967-0661(97)10029-6

http://dx.doi.org/10.1016/S0967-0661(97)10029-6

Publisher:
Pergamon and Elsevier on behalf of the International Federation of Automatic Control (IFAC)

Pergamon

Control Eng. Practice, Vol. 5, No.12, pp. 1739-1745, 1997

00967-0661/97 $17.00+0.00

PII:S0967-0661(97)10029-6

ON IMPROVING PHYSICAL SELECTIVITY IN THE TREATMENT OF CANCER: A SYSTEMS MODELLING AND OPTIMISATION APPROACH

O.C.L. Haas*, K.J. Burnham* and J.A. Mills**

**Control Theory and Applications Centre, Coventry University, UK (cta@coventry.ac.uk)*
***Department of Clinical Physics and Bioengineering, Walsgrave Hospital, UK*

(Received July 1997; in final form August 1997)

Abstract: This paper presents the results arising from a practical implementation of a novel hybrid optimisation scheme, used to solve the inverse problem in radiotherapy treatment planning (RTP). A matrix-based beam model which has been developed making use of a control systems modelling approach is used, together with a hybrid optimisation scheme. Patient-specific compensator profiles are deduced from the intensity modulated beam profiles obtained from the hybrid scheme, with use being made of an exponential attenuation factor coupled with a point spread convolution function to account for the scatter in the compensator. A good agreement between the predicted and actual conformational distributions is achieved.

Keywords: Genetic algorithms, geometric approaches, inverse problem, iterative methods, least squares methods, multiobjective optimisation, physics, systems methodology.

1. INTRODUCTION

Improved treatment of cancer can be achieved either by adding substances whereby the sensitivity of diseased cells to radiation is increased, or by improving the physical selectivity of the treatment by conforming the dose delivered as closely as possible to the dose prescription. The approach presented in this paper differs from previous work in that a global view of the optimisation of radiotherapy treatment is considered. In particular, all the important aspects of the optimisation are taken into account. Following the steps of treatment planners, the algorithm starts with the optimisation of the beam orientation, prior to optimising the beam intensity modulation, and finally adapts the theoretical solution obtained with an analytical technique derived from iterative least squares (ILS) combined with a parallel beam model to a practicably implementable solution. This requires the actual beam divergence as well as the compensator itself to be taken into account. The aim of the prescription is to deliver a suitably high dose to the diseased region within the prescribed target area (PTA), whilst sparing the organs at risk (OAR) and minimising the dose delivered to the other healthy tissues (OHT). To improve the solution further, additional criteria such as the minimisation of hot spots created by unbalanced plans have been developed (Haas, et al., 1996a). Optimising a treatment to improve its physical selectivity involves the determination of both the optimal beam orientation, as well as the optimal intensity modulated beam (IMB) profiles. The latter involves the solution of the so-called "inverse problem" in RTP (Brahme, 1988). In previous work the inverse RTP problem has been solved either with analytical techniques (Holmes and Mackie, 1994) or with random search techniques such as simulated annealing (Webb, 1991). However, most optimisation methods have not considered practical implementation problems, and have rarely been physically demonstrated (Bortfeld, et al., 1994). In

this work a hybrid optimisation technique has been adopted, in which use is made of both analytical and random search techniques.

IMBs can be realised with complex dynamic techniques based on the use of multileaf collimators (MLCs), or static techniques making use of patient-specific compensators (PSCs). Although MLCs have been favourably compared to traditional beam-shaping techniques (Fernandez, et al., 1995), they are not used dynamically under clinical conditions. Therefore, in this work the PSCs, which are deduced from the optimised IMB profiles, are used to modulate the beam intensities.

2. BEAM MODELLING

Two-dimensional parallel and divergent pencil beam models have been developed around a matrix formulation that lends itself to the solution of the inverse problem. The parallel formulation is used solely with ILS, whilst the divergent model is used to advantage with forward-solving methods, such as genetic algorithms (GAs).

The model developed here separates the dose delivered by a given beam into primary and scatter contributions. The primary dose depends only on the depth for a homogeneous medium, and can be computed using density-weighted path lengths or equivalent path lengths for an inhomogeneous medium (Redpath and Aspratakis, 1994). The scatter contribution attempts to account mainly for the Compton scattering effect due to the incoming photons interacting with the body structures (Attix, 1986). In addition, account is taken of in-air-profile, penumbra and patient contour correction (Haas, 1997).

Each beam involved in a treatment plan can be decomposed into elemental pencil beams. Each pencil beam can be modified independently to produce a set of IMBs from which the resulting dose **d** is given by

$$\mathbf{d} = \Phi\,\mathbf{b} \tag{1}$$

where **b** is the vector of IMBs and Φ is the dose calculation matrix, details of which may be found in (Haas, 1997).

In order to make use of the beam model in the prediction and delivery of conformal treatment, it has been tuned to replicate 6 MV and 25 MV photon beams that are in use at Walsgrave Hospital, NHS Trust, Coventry.

The behaviour of a beam interacting with the human body structures can be described or characterised in terms of central axis percentage depth dose (%DD) and the isodose profiles at various depths. Such features provide information regarding the attenuation of the beam with respect to depth and characterises the variation of the dose across the field respectively. Because the density of human body structures is close to that of water, it is common practice to assess beam models using a water phantom, see Figure 1.

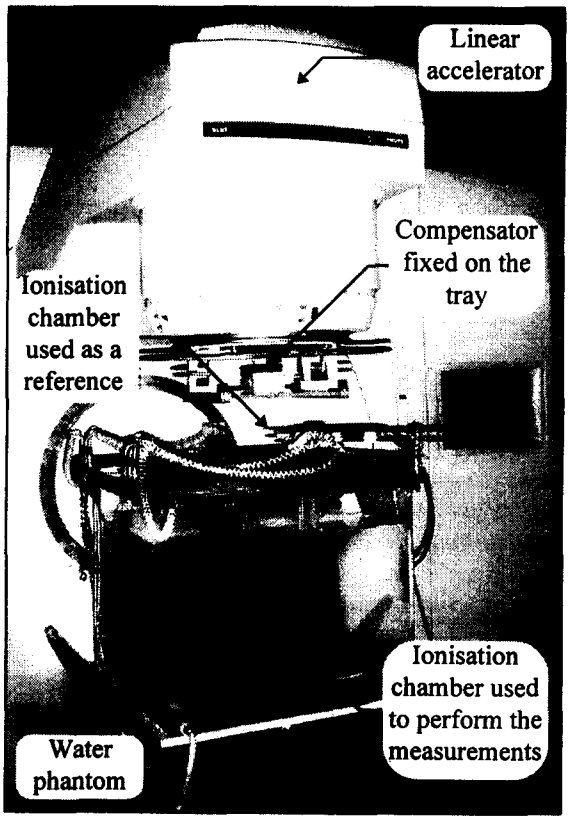

Fig. 1. Water phantom used to assess the beam model for a homogeneous medium at Walsgrave Hospital, NHS Trust, Coventry.

The dose is measured using an ionisation chamber immersed in a water phantom. The process involves traversing the ionisation chamber across the field (beam width) at depths of 1.5, 9.5, 14 and 25 cm.

Wedge-shaped compensators are routinely used in the delivery of radiotherapy treatment to attenuate the beams. Whereas the gradient across a field shaped by IMBs is likely to be non-uniform, a wedge-shaped compensator gives rise to a constant gradient across the field. In order to demonstrate the ability of the beam model to replicate dose distributions formed by standard wedges and IMBs, a wedge-shaped compensator that is shorter than the field size (FS) has been used, see Figure 2.

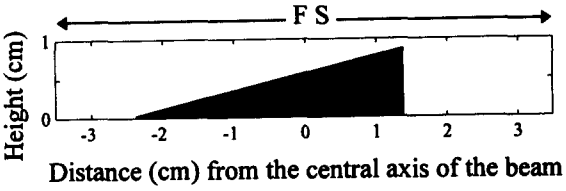

Fig. 2. Illustrating a wedge-shaped compensator located on the tray of the linear accelerator.

Note that due to the divergence of X-ray photon beams, a field size (FS) of 6.6 cm × 6.6 cm at the tray level, positioned at 66.0 cm from the beam source, corresponds to a FS of 10.0 cm × 10.0 cm at a source-to-skin distance (SSD) of 100.0 cm.

With reference to Figure 3, it can be observed that although the wedge-shaped compensator has a vertical edge between the highest point of the compensator and the tray, the isodose plot shows a much smoother increase in the dose. This limits the type of profile that can be physically achieved with PSCs. Clearly, this is required to be taken into account, both in the optimisation process as well as in the implementation of PSCs.

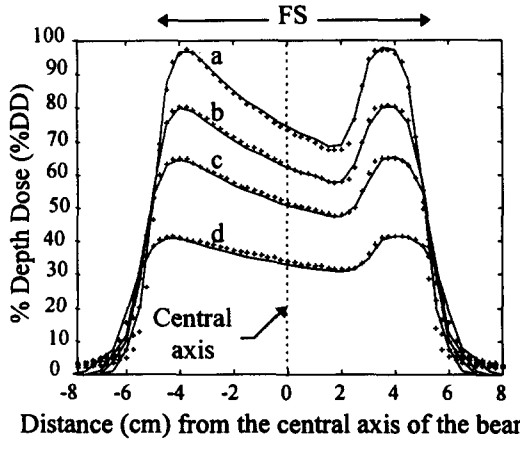

Fig. 3. Comparison between measured '+' and calculated '-' isodose plots at depth a=1.5 cm, b=9.5 cm, c=14.0 cm and d=25.0 cm for a 6 MV photon beam with a wedge-shaped compensator inserted into the beam path.

The model is able to reproduce the dose distribution adequately, with the mean absolute error expressed as a percentage between the calculated and the measured dose being approximately 1.8%.

3. USE OF MULTIPLE BEAMS IN RTP

The first step in any RTP procedure is for the treatment planner/clinician to select the number and orientation of the beams. The increased complexity of treatment plans, particularly in conformation therapy, where many beams may be involved, has provided the motivation to develop fast and robust methods for optimising the beam orientation.

The overall optimisation of the orientation and the intensity modulation of all the beams involved in a treatment plan is illustrated using a typical case involving a prostate cancer in the pelvic region. Figure 4 shows a typical computed tomography (CT) slice, in which the regions of interest (ROI) for the planning stage are outlined. The ROI are the PTA, the OAR and the OHT.

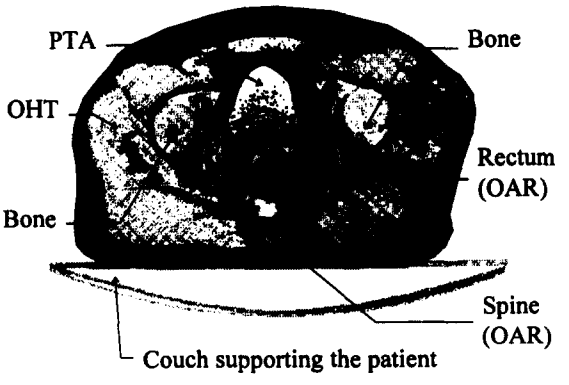

Fig. 4. Typical CT slice of a pelvic region with manual delineation of the ROI.

In (Haas, et al., 1996b) a geometrical formulation of the coplanar beam-orientation problem, coupled with a form of multiobjective genetic algorithm (MOGA), is introduced. Figure 5 shows a typical set of non-dominated solutions, referred to as a "Pareto-optimal set" (Fonseca, 1995; Steuer, 1986) determined by the MOGA.

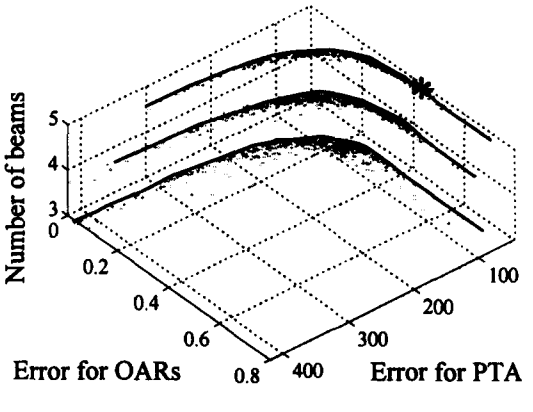

Fig. 5. Pareto-optimal set used in RTP.

The solutions are displayed for three normalised objectives; namely cost in the PTA, cost in the two OARs, and the number of beams. The point marked '*' represents a solution selected for its high degree of conformation with the PTA. The optimised beam orientation for this solution is shown in Figure 6.

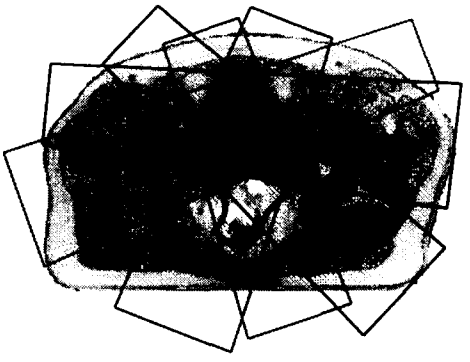

Fig. 6. Optimal beam orientation corresponding to the solution marked '*' in Fig. 5.

Note that although several beams overlay the two OARs, a reasonably low dose should be received. This is due to the fact that the beam entry points are chosen to be closer to the PTA than to the OARs (Haas, et al., 1996b).

4. HYBRID OPTIMISATION SCHEME

The aim of the hybrid scheme is to exploit the desirable features of analytical ILS and random search MOGA techniques. Initially ILS is used to determine a good solution in only a few iterations, and a MOGA is subsequently used to adapt the solution whilst allowing additional freedom in the choice of objective function employed.

The cost function utilised within the ILS scheme minimises:

$$\mathbf{J}_{(b)} = \{ \alpha C_{PTA} + \beta C_{OAR} + \delta C_{OHT} \} \quad (2)$$

where C_{PTA}, C_{OAR} and C_{OHT} are defined as:

$$C_{PTA} = [\delta_{PTA} - \mathbf{d}_{PTA}]^T [\delta_{PTA} - \mathbf{d}_{PTA}] \quad (3)$$

$$C_{OAR} = [\delta_{OAR} - \mathbf{d}_{OAR}]^T [\delta_{OAR} - \mathbf{d}_{OAR}] \quad (4)$$

$$C_{OHT} = [\delta_{OHT} - \mathbf{d}_{OHT}]^T [\delta_{OHT} - \mathbf{d}_{OHT}] \quad (5)$$

with δ representing the prescribed dose and $\mathbf{d}$ the calculated (or predicted) dose for each ROI. Note that $\alpha, \beta, \gamma \in \Re$ are the objective weightings, chosen such that $\alpha \cong \beta >> \gamma$. This ensures that a high dose, according to prescription, is delivered to the PTA, with a minimum dose to the OAR and a low dose to the OHT (Haas, et al., 1996a).

In the approach developed in this work, each beam is considered as a 'semi-independent' system. This is believed be advantageous since a computationally complex problem is divided into N_{beam} smaller problems. The inverse problem is iteratively solved for each beam, such that the overall search strategy can be separated into parallel and sequential processes.

4.1 Parallel processes:

- Extract the individual error allocated to each beam.
- Solve each inverse problem

$$\mathbf{b}_i = \mathbf{b}_{i-1} + \left[\mathbf{H} - \lambda diag\mathbf{H}\right]^{-1} \Phi^T [\mathbf{W}[\delta - \mathbf{d}]] \quad (6)$$

  where $\mathbf{b}_i$ is the current estimate of the IMB vector that is deduced from the previous estimate $\mathbf{b}_{i-1}$, with $\mathbf{H}=\Phi^T\Phi$, and $\lambda \geq 0$ is chosen as $\lambda = 0.6$. The adaptive weighting matrix $\mathbf{W}$, the form of which is fully detailed in (Haas, 1997), is a diagonal matrix in which the elements are functions of both the errors and the ROI considered. The aim is to modify the initial objective weightings in order to vary their importance according to the dose variation between grid points belonging to the same ROI.
- Calculate the beam dose distribution, i.e. rotate and map the resulting dose distribution onto the total dose matrix grid.

4.2 Sequential processes:

- Sum all the dose distributions.
- Calculate the error between prescribed and calculated dose.
- Allocate a portion of the error to each beam.

Making use of this adaptive error-weighting scheme combined with ILS gives rise to the isodose contour plot shown in Figure 7.

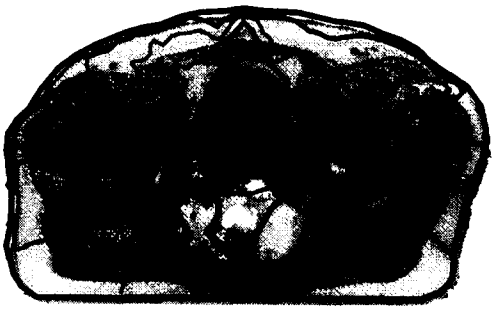

Fig. 7. Dose distribution obtained using the ILS scheme with adaptive weighting of the error.

Note that whilst the dose within the PTA is within specification (100% ±5%), a very low dose is delivered to the OARs (i.e. between 10% and 30%).

The MOGA approach, which is used for refining the solutions obtained from ILS, is based on a rank-based fitness assignment (Fonseca, 1995). All the non-dominated solutions are assigned a rank of unity.

The rank of the other solutions is given by the number of solutions by which these solutions are dominated. In order to focus the search in the most promising regions of the current non-dominated solutions, those with a similar rank are differentiated by making use of the following fitness function:

$$Fitness = 2 - SP + 2(SP-1)\,(R + f(C_{PTA}, C_{OAR}, C_{OHT}) / max(f(C_{PTA}, C_{OAR}, C_{OHT})) - 1)\,/(Nind-1) \quad (7)$$

where $f(C_{PTA}, C_{OAR}, C_{OHT}) = (\alpha C_{PTA} + \beta C_{OAR} + \delta C_{OHT})$ (8)

where α, β and γ represent the relative importance of each of the objectives, $SP \in \Re$, $1 \le SP \le 2$ is the selective pressure, R is the rank of the individual, $Nind$ is the number of individuals in the population and $max(f(C_{PTA}, C_{OAR}, C_{OHT}))$ is the maximum value of (5). The selective pressure is required to be kept low to avoid premature convergence. At each generation the best solution for each objective is recorded and compared to the solution that offers the best compromise.

5. DETERMINATION OF COMPENSATOR PROFILES

The beam model developed here does not take into account the interaction of radiation outside the body structures. It is therefore necessary to determine a relationship between the beam profile and the compensator thickness. The compensators are manufactured in a tin zinc alloy (MCP 200) with a density of 7 10^3 kg/m^3. The primary attenuation in the compensator is modelled as an exponential function of the thickness. Similar to (Jursinic, et al., 1994) the thickness h of compensators is given by:

$$h = \frac{1}{\mu} \ln\left(\frac{D_{\%}}{100}\right) \quad (9)$$

where $D_{\%}$ is the IMB profile at the point of equilibrium (Attix, 1986), μ is the linear attenuation coefficient and h is the height (or thickness) of the compensator. However, this relationship does not account for the scatter within the compensator, which has a smoothing effect. This is modelled as a point spread function convolved with the primary component $p = 100e^{-\mu h}$ and, in an iterative manner, the compensator profile which fits the predicted IMB profile is deduced (Haas, 1997).

With reference to the experimental verification of the approach involving a five-field RTP considered in Section 6, the predicted IMB and corresponding compensator profiles for Beam 2 in the plan are given in Figures 8 and 9 respectively.

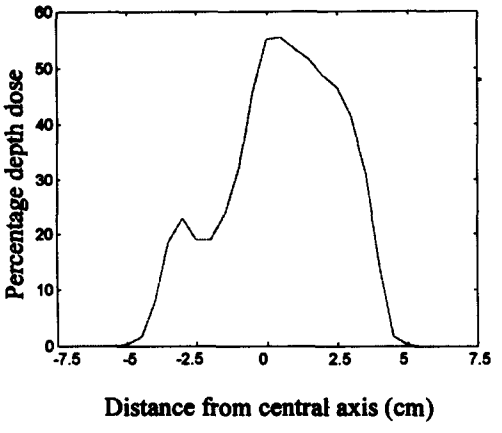

Fig. 8. Optimised IMB profile for Beam 2.

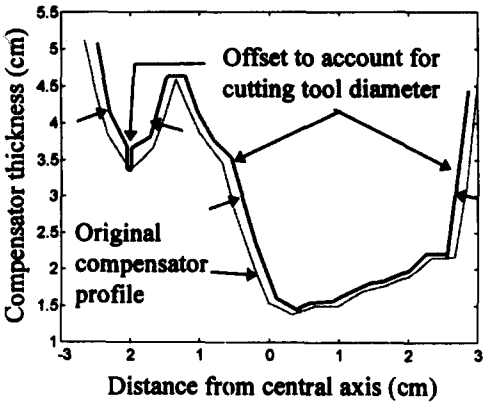

Fig. 9. Compensator profile for Beam 2, with correction for tool path.

The compensators are manufactured from the given compensator profiles using an industrial standard computer numerically controlled (CNC) machine and tool path generating code. In order to account for the diameter of the tool (6 mm) it is necessary to offset the tool path both on the left and on the right. The resulting compensators are shown in Figure 10.

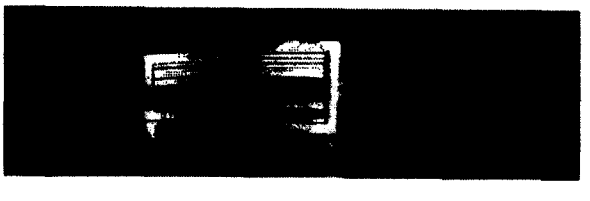

Fig. 10. Illustrating the five compensators manufactured with a CNC machine at Waslgrave Hospital, NHS Trust, Coventry.

6. EXPERIMENTAL VERIFICATION

In order to verify the overall approach of optimisation of beam orientation and IMB profiles, use is made of a semi-anatomical torso phantom, for which ROI outlines are shown in Figure 11.

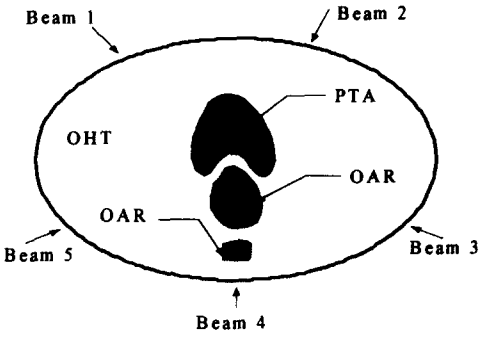

Fig. 11: Torso phantom contour with ROI outlined.

The ROI have been outlined to replicate the main anatomical structures encountered in the pelvic region, see Figure 4. A concave PTA, taken as being the prostate, has been outlined, and an OAR, taken as the rectum, is located in the concavity of the PTA. Another OAR, taken as the spine, is also considered .

The prescription requires that a high dose be delivered to the PTA whilst a low dose is to be received by the OARs, in this case the rectum, with a very low dose to the spine. The beam orientation has been selected such that it conforms well to the PTA, with limitation of the dose in the OARs being taken care of by optimising the IMB profiles.

The torso phantom is set up exactly as a patient would be, with a film positioned as a 'sandwich' through its centre, see Figure 12. It is then sealed to ensure that it remains clear until it is exposed to radiation.

The film represents a slice through the torso and, therefore, when it is exposed to the combination of IMBs produced by the compensators, it provides a density variation proportional to the dose received. The resulting dose distribution was then measured by scanning the film and this revealed a conformal dose distribution.

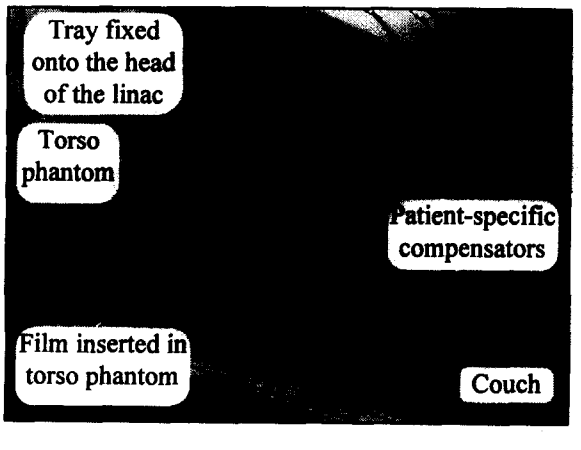

Fig. 12. Illustrating the experimental set-up at Walsgrave Hospital, NHS Trust, Coventry.

In order to determine the appropriate beam weightings it is necessary to take measurements using each compensator in order to ensure the correct exposure from the treatment machine is achieved. Linear accelerators used at Walsgrave Hospital are calibrated such that one monitor unit (mu) corresponds to a dose of 1 cGy, known as the calibration c, delivered at the point of equilibrium (Attix, 1986) by a 10 cm by 10 cm field, with an SSD=100 cm. The number of monitor units to be set for the i^{th} beam, M_i is then required to be calculated with respect to the calibration condition such that:

$$M_i = \frac{D_i}{o_i \left(\frac{100}{SSD}\right)^2 c} \tag{10}$$

where

$$D_i = D_{ISO} \frac{T_i}{T_{ISO}} \tag{11}$$

$i=1...N_{beam}$, where $N_{beam} = 5$ in this work.

Note that D_i corresponds to doses measured at the point of equilibrium (3.5 cm depth for 25 MV) for each beam and T_i corresponds to the numerical value in terms of %DD at the same point in the predicted dose distribution. The subscript *ISO* refers to the point of intersection of all the beams, which is a single point known as the isocentre. In the first experiment D_{ISO} = 60 cGy, T_{ISO}=100, T_i, i=1...5 are 43, 41, 32, 40, 27 respectively, leading to M_i, i=1...5 as 32, 31, 18, 27, 20 respectively (Haas, 1997).

The delivery of a conformal treatment requires an accurate positioning of the compensators with respect to the patient. In order to achieve this, it is necessary to position the torso phantom such that the central axis of each beam passes through the isocentre of the PTA. The beams can then be rotated about the isocentre to their respective positions. Note that in order to spare the spine and to reduce the compensator height, Beam 4 is delivered as two small fields.

Isodose contour plots for predicted and measured dose distributions are shown in Figures 13 and 14 respectively. The isodose plots shown in Figure 13 have been calculated, with use being made of the ILS routine to determine a good first approximation of the beam profiles, that were then adapted to a divergent beam model with a MOGA.

With use being made of the optimisation procedure, it is possible to predict the resulting dosimetry from a given optimised treatment plan. Figure 13 shows the predicted dose distribution for the practical test case considered.

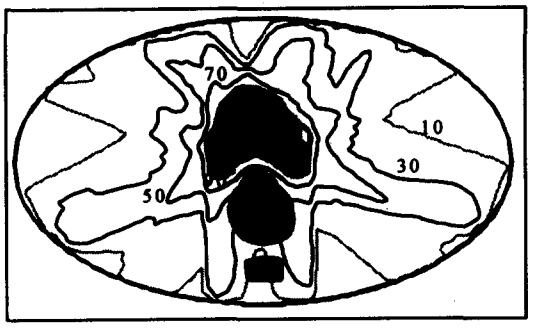

Fig. 13. Predicted isodose contour plot with use being made of the hybrid optimisation scheme.

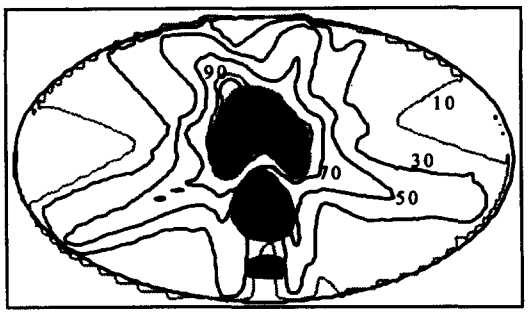

Fig. 14. Digitised isodose contour plot obtained from the development of a slow film.

The results recorded on a radiosensitive film, and subsequently digitised, show a sparing of the OAR that could not be achieved using conventional techniques, see Figure 14. These results, first reported in (Haas, 1997), constitute the first successful practical demonstration of the systems modelling approach developed at Coventry University, in collaboration with Walsgrave Hospital NHS Trust, to deliver intensity modulated radiation therapy.

7. CONCLUSIONS

The paper has presented a practical verification of a global approach to the optimisation of X-ray photon beam orientation and intensity modulation for radiotherapy treatment. A solution to the beam orientation problem, which has been optimised on a geometrical basis, together with a hybrid approach for optimising intensity modulation have been demonstrated practically. A relationship between the optimised beam profiles and the compensator profiles has been proposed, thus allowing the manufacture of the compensators with a CNC machine.

The overall results obtained indicate that the acknowledged potential of intensity modulated radiation therapy can be realised. The results would suggest that use of conformal radiotherapy in the treatment of cancer is a realistic clinical option and should, therefore, be taken seriously.

REFERENCES

Attix, F.H. (1986). *Introduction to Radiological Physics and Radiation Dosimetry*, John Wiley & Sons, USA.

Bortfeld, T., D. Kahler, T. Waldron and A. Boyer (1994). X-ray field compensation with multileaf collimators, *Int. J. Radiation Oncology Biol. Phys.*, **28** (3) pp. 723-730.

Brahme, A. (1988). Optimisation of stationary and moving beam radiation therapy techniques, *Radiotherapy and Oncology*, **12**, pp. 129-140.

Fernandez, E.M., G.S. Shentall, W.P.M. Mayles and D.P. Dearnaley (1995). The acceptability of a multileaf collimator as a replacement for conventional blocks, *Radiotherapy and Oncology*, **36**, pp. 65-74.

Fonseca, C.M. (1995). *Multiobjective Genetic Algorithms with Application to Control Engineering Problems*, PhD Thesis, University of Sheffield, UK.

Haas O.C.L., K.J. Burnham, M.H. Fisher and J.A. Mills (1996a). Implementation of hot spot correction schemes for use in optimisation algorithms for conformation therapy, *Radiology UK 96*, Birmingham, UK, *British Journal of Radiology*, Suppl. to vol. **69**, pp. 100.

Haas O.C.L., K.J. Burnham, M.H. Fisher, J.A. Mills and C.R. Reeves (1996b). Genetic algorithms applied to beam orientation in radiotherapy, *Fourth European Congress on Intelligent Techniques and Soft Computing EUFIT 96*, Aachen, Germany, pp. 2050-2055.

Haas, O.C.L. (1997). *Optimisation and Control Systems Modelling in Radiotherapy Treatment Planning*, PhD Thesis, Coventry University, UK.

Holmes, T. and R.T. Mackie (1994). A comparison of three inverse treatment planning algorithms, *Phys. Med. Biol.* **39**, pp. 91-106.

Jursinic, P.A., B. Podgorsak and B.R Paliwal (1994). Implementation of a three-dimensional compensating system based on computed tomography generated surface contours and tissue inhomogeneities, *Med. Phys.*, **21**, pp. 357-365.

Redpath, A.T. and M.M. Aspratakis (1994). A beam model for three-dimensional photon treatment planning, Proc. *XIth Int. Conf. on the Use of Computers in Radiation Therapy* (ICCR), Manchester, UK, pp. 236-237.

Steuer, R.E. (1986). *Multiple criteria optimization: Theory, Computation, and Application*, John Wiley & Sons, Singapore.

Webb, S. (1991). Optimisation by simulated annealing of three-dimensional, conformal treatment planning for radiation fields defined by a multileaf collimator, *Phys. Med. Biol.*, **36**, pp. 1201-1226.